Utah State University
DigitalCommons@USU

All Physics Faculty Publications | Physics, Department of

1-1-2000

# Measurements of Electronic Properties of Conducting Spacecraft Materialswith Application to the Modeling of Spacecraft Charging

W. Y. Chang

JR Dennison
*Utah State University*

Parker Judd

Recommended Citation
W.Y. Chang, JR Dennsion and Parker Judd, "Measurements of Electronic Properties of Conducting Spacecraft Materials with Application to the Modeling of Spacecraft Charging," Paper AIAA-2000-0870, Proceedings of the 38th American Institute of Aeronautics and Astronomics Meeting on Aerospace Sciences, (Reno, NV, 2000).

This Conference Paper is brought to you for free and open access by the Physics, Department of at DigitalCommons@USU. It has been accepted for inclusion in All Physics Faculty Publications by an authorized administrator of DigitalCommons@USU. For more information, please contact digitalcommons@usu.edu.

UtahStateUniversity
MERRILL-CAZIER LIBRARY

# Measurements of Electronic Properties of Conducting Spacecraft Materials with Application to the Modeling of Spacecraft Charging

W. Y. Chang, J. R. Dennison and Parker Judd
Physics Department, Utah State University, Logan, Utah

**Abstract**

This paper describes the results of the first stage of this project, measurements of the electronic properties of conducting spacecraft materials. We begin with a description of the required measurements and specifics of the experimental methods used. A complete list of the conducting materials studied, justification of their selection for study, and a summary of the important results of the measurements is presented. This is followed by detailed measurements and analysis for one representative conductor, namely polycrystalline Au. We end with a description of incorporation of these measurements into the NASCAP database.

## INTRODUCTION

Many spacecraft system anomalies and component failures are known to result from spacecraft charging which is due to the bombardments of spacecraft by energetic electrons, ions, and photons in natural space environment [*Hastings and Garrett,* 1996; *Bedingfield et al.,* 1996; *Leach et al.,* 1995]. To assist spacecraft designers in accommodating and mitigating the harmful charging effects on spacecraft, NASA has developed an extensive set of engineering tools to predict the extent of charging in various spacecraft environments (for example, NASCAP/LEO, NASCAP/GEO, and POLAR) [*Mandell et al.,* 1993]. However, current NASCAP databases lack electronic properties of most spacecraft materials in use (only nine basic materials are presently incorporated) and many new spacecraft bulk materials and coatings need to be characterized. In an effort to improve the reliability and versatility of these models, the NASA Space Environments and Effects (NASA/SEE) Program has funded a study to measure the electronic properties of spacecraft materials related to NASCAP parameters [*Dennison*, 1998]. The objectives of the study are (i) to provide more accurate measurements together with sufficient materials characterization and (ii) to significantly extend the database to include a wider range of materials that are more representative of the myriad materials used in spacecraft design and to incorporate newly developed materials.

This paper describes the results of the first stage of this project, measurements of the electronic properties of conducting spacecraft materials. We begin with a description of the required measurements and specifics of the experimental methods used. A complete list of the conducting materials studied, justification of their selection for study, and a summary of the important results of the measurements is presented. This is followed by detailed measurements and analysis for one representative conductor, namely polycrystalline Au. We end with a description of incorporation of these measurements into the NASCAP database.

## EXPERIMENT

The NASCAP code designed to model spacecraft charging uses 19 parameters to characterize the electronic properties of a given material [*Mandell et al.,* 1993]. For each sample studied, measurements are made to determine these 19 parameters. Table I identifies the experimental methods and apparatus employed to determine these physical properties. The measurements can be grouped under three headings:

*(i) sample characterization*, used to fully identify the specific materials tested and to allow end users to more accurately assess which material is most closely related to their specific spacecraft materials;

*(ii) conduction related properties*, used to model the response of materials to accumulated charge; and

*(iii) electron emission* (induced by electrons, ions, photons) which determine a material's response to space environment fluxes.

The measurement methods and instrumentation specific for conducting samples are described below in more detail for each of these three groups. A number of additional property measurements, highlighted in italics in column three of Table I, are included in the study; the intent of these additional measurements is to extend the description of the electronic properties of the materials with the goal of improving the modeling of spacecraft charging in future codes. Further details of the instrumentation used for these measurements is found elsewhere [*Chang et al.*, 1999].

### *Sample Preparation and Characterization*

Each conducting 1 cm diameter disk was polished using 0.25 μm diamond paste and cleaned using standard solvents prior to insertion into the vacuum chamber. Surface morphology was characterized *ex situ* using optical microscopy, scanning electron microscopy (SEM), and scanning tunneling and atomic force microscopy (STM/AFM). The disks were subsequently mounted on a sample carousel in a UHV chamber (base pressure $<10^{-10}$ Torr). *In situ* characterization of surface morphology was accomplished with SEM and surface contamination was monitored with Auger electron spectroscopy (AES).

### *Conduction Related Properties*

A standard four-point probe was used for *ex situ* measurements of bulk and surface conductivity.

**Table I. Methods and apparatus used for properties measurements related to NASCAP modeling parameters.**

| Property Category | Measured Property (Methods and Apparatus) | Related NASCAP Parameters [Mandell et al. 1993, *] |
|---|---|---|
| Sample Character-ization | Density (Gravimetric) | Density; $\rho$ [9,19]. |
| | Bulk Composition (AA, ICP) | Mean atomic number <Z> [4] and weight <A> [10]. |
| | Surface contamination (*in situ* AES, AES mapping) | |
| | Surface morphology (*in situ* SEM.; *ex situ* STM/AFM, SEM, optical microscopy) | |
| | Coating thickness (*in situ* HEED; *ex situ* STM/AFM, optical microscopy) | Dielectric film thickness; d [2]. |
| Conduction Related Properties | Dielectric constant (*ex situ* capacitive measurements) | Relative dielectric constant; $\epsilon_r$ [1]. |
| | Bulk and surface conductivity (*in situ* and *ex situ* 4-point resistance probe measurements) | Bulk conductivity; $\sigma_o$ [3]. Surface resistivity; $\rho_s$ [14]. *Temperature dependence of conductivity.* |
| | Electrostatic discharge (*in situ* I-V profiles of non-conducting films on conducting substrates) | Maximum potential before discharge to space; $V_{max}$ [15]. Maximum surface potential difference before dielectric breakdown discharge; $V_{punch}$ [16]. |
| | High-energy plasma radiation-induced conductivity (*in situ* 4-point probe measurements for flux of monoenergetic electrons for non-conductive samples) | Two parameter fit of radiation-induced conductivity, $\sigma_r$; k and $\Delta$ [17, 18]. |
| Electron-Induced Emission | SE/BES total yields versus incident electron energy (Emission current for flux of monoenergetic electrons from 100 eV to 30 keV). | Maximum SE yield; $\delta_{max}$ [5]. Energy for $\delta_{max}$; $E_{max}$ [6]. Effective atomic number, $Z_{eff}$, for $\eta(E_o)$ [4].*Extended parameter fits for $\delta(E_o)$ and $\eta(E_o)$. Incident angle dependence of $\delta(E_o)$ and $\eta(E_o)$.* |
| | Stopping power data. | Four-parameter bi-exponential range law fit for PE energy range derived from stopping power data; $b_1$, $n_1$, $b_2$, $n_2$ [7-10]. |
| | Energy- and angle- resolved BS/SE cross sections. (Cross sections using rotatable Faraday cup retarding field analyzer.) | *Parameters for Lambert cosine law fit of angular resolved cross sections [Nickles et al 1999]. Parameters for Chung and Everhart [1974] model of energy resolved cross section. Parameters for coupled energy-angle resolved cross section [Nickles et al 1999; Chang et al, 2000].* |
| Ion-induced Emission | Total electron yield versus incident ion energy (Emission current form flux of monenergetic He ions at 500 eV to 5 keV) | SE yield due to 1 keV proton impact; $\delta^H$(1keV) [11]. Incident proton energy for $\delta^H_{max}$; $E^H_{max}$ [12]. *Ion energy dependence of emitted electron yields.Energy spectra of emitted electrons. Species dependance of ion yields.* |
| Photon-induced Emission | Total electron yield versus incident photon energy (Emission current for flux of monoenergetic photons from discharge lamps ) | Total electron yield from solar spectrum [13]. *Photon energy dependence of emitted electron yields. Energy spectra of emitted electrons.* |

* The numbers of the materials database parameters used in the current version of NASCAP are indicated in square brackets. Proposed additions to the database are indicated in italics.

*Electron-Induced Emission Measurements*

The total backscattered electron (BSE) yield $\eta$ and secondary electron (SE) yield $\delta$ were measured for normal incident electron beams as functions of incident energy over a range of $\lesssim$100 eV to 30 keV. A hemispherical grid retarding field detector (see Fig. 1) was used to measure emission current. By ramping the grid bias, energy spectra of the emitted electrons were also measured using this detector. Two electron sources were used: (i) a low energy ($\lesssim$50 eV to 3 keV) electron gun, based on a design by Conrad [*Cao and Conrad, 1989*], that used unipotential operation with a $LaB_6$ thermionic cathode to produce a small spot size (~100 μm) and reasonable currents (>25 nA) even at low beam voltages with resolutions of $\Delta E/E<2x10^{-4}$ and (ii) a HEED electron gun with a highly collimated (<20 μrad divergence) and well focused (~20 μm diameter), intense (0.1 nA to 10 μA), monoenergetic ($\Delta E/E<2\cdot10^{-4}$) electron beam from 3 to 30 keV energies. Extension to these higher incident energies are essential to simulate

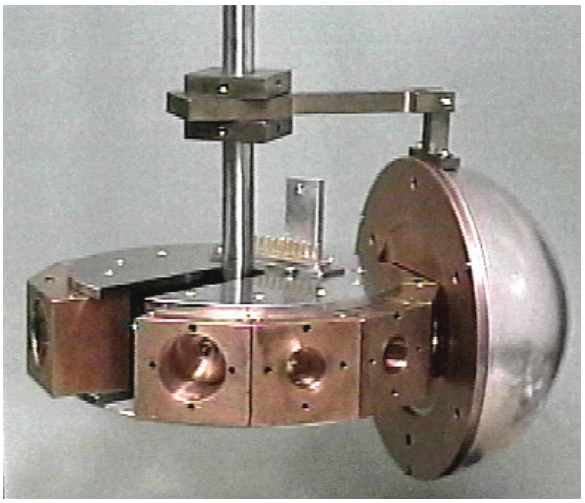

**Fig.. 1** Stage carousel and retarding field energy analyzer.

spacecraft charging [*DeForest 1972, Frooninchx 1991, Groosenhoven 1983, 1985, Katz 1986*] which has major contributions from precipitation of energetic electrons from the magnetosphere along Earth's magnetic field lines; such precipitation has been positively linked to severe spacecraft charging events *[Frooninchx 1991,1992; Groosenhoven 1985*].

Measurement of the total SE yield allowed reliable determination of the maximum SE yield $\delta_{max}$ and the energy $E_{max}$ at which $\delta_{max}$ occurred. These two parameters are used in NASCAP to model the SE yield as a function of incident energy. Four additional parameters, $b_1$, $n_1$, $b_2$, $n_2$, are used to describe the shape of the reduced yield curve $\delta(E_0)/\delta_{max}$ vs. $E_o/E_{max}$ . They are typically determined from a bi-exponential range law fit for PE energy range derived from stopping power data *[Mandell, 1993*]. They can also be determined directly from fits to the SE yield curve; in this case $b_2$ and $n_2$ describe the shape of the high energy tail of the curve while $b_1$ and $n_2$ model the region from $E_{max}$ to a few keV incident energies [*Mandell, 2000; Chang 2000*]. In addition, we determined alternate fits to the reduced yield curve using a number of other models which potentially provide more accurate models, particularly in the high energy tail, including those by Sternglass [*1957*], Schwartz [*1990*], and Dionne [*1975*]. Angle- and energy-resolved spectra $\eta(E,\alpha)$ and $\delta(E,\alpha)$ were also measured for selected conducting materials. The intent was to provide representative data for these cross sections that could be incorporated into future charging codes. It has been determined that under certain circumstances encountered in near-earth orbits incorporating more omplete knowledge of the energy- and angle-resolved spectra of SE is necessary to fully model how SE emission and spacecraft charging are affected by re-adsorption of low energy electrons by the emitting surface

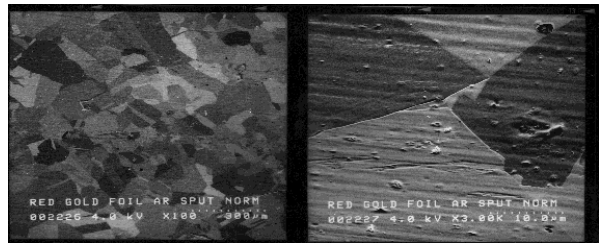


**Fig.. 2** SEM image of Ar sputtered polycrystalline Au.

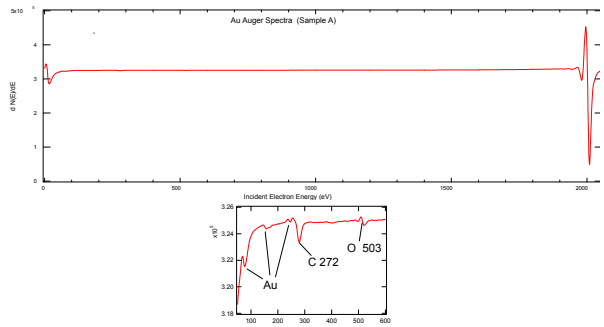


**Fig. 3.** AES spectra of C contaminated polycrystalline Au.

or adjacent surfaces in the presence of charge-induced electrostatic fields [*Nickels et al, 1999*].

Angle-resolved measurements were made in a smaller UHV chamber, dedicated primarily to angle-resolved SE emission measurements [*Davies 1996; Davies 1999; Chang et al., 1999*]. A custom retarding field analyzer Faraday cup type detector, continuously rotatable about the sample, was used to obtain angle-resolved SE yield and spectra for normally incident electrons over a range of emission angles of $-16° < \alpha < +76°$ [*Nickles et al.*, 1999]. Angular resolution of the instrument is ~1.5° and the energy resolution is 0.5 eV ± 0.03% of the incident beam energy [*Davies, 1999*].

The angle-resolved distributions were fit with a theoretical Lambert cosine dependence of secondary electron yield, $\delta(\Theta)=\delta(0)\cos(\Theta)$ [*Nickles et al., 1999*]. Energy-resolved distributions were fit to the Chung and Everhart [*1974*] model for energy-resolved cross sections. Coupled energy-angle resolved cross sections were fit to a modified Chung and Everhart expression [*Nickles et al., 1999; Chang et al., 2000*].

*Ion-Induced Emission Measurements*

Total electron yield due to ion bombardment as a function of incident ion energy are measured using the same hemispherical grid retarding field analyzer used for SE/BSE emission measurements. This detector allows measurement of the energy spectra of the emitted

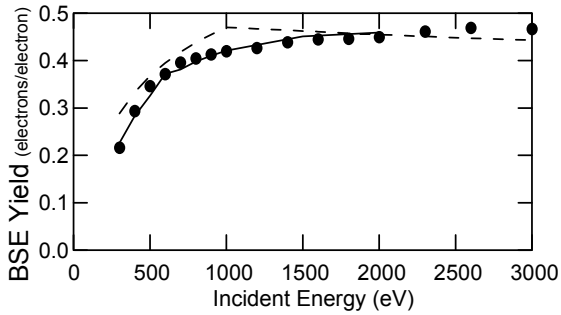


**Fig. 5.** Total backscattered yields vs incident energy for polycrystalline Au.

electrons. A cold cathode ion gun is used as the source for monoenergetic He ions over the range of 500 eV to 5000 eV. The sample is biased to -20 eV to repel SE which would contaminate the emission measurements.

As modeling parameters for ion-induced electron emission, NASCAP requires the SE yield due to 1 keV proton impact, $\delta^H$(1keV), and the incident proton energy for $\delta^H_{max}$, $E^H_{max}$.. Our measurements do not go to high enough energies to determine $E^H_{max}$, which is typically near 100 keV. However, the range of energies over which measurements are made were sufficient to determine an approximate value through extrapolation. Our measurements were done with He rather than incident protons, however this should not present a significant problem as NASCAP assumes that the emission is the same for all ion species, independent of mass [*Mandell et al., 1993*]. Measurements are planned to study the dependence of $\delta^H_{max}$, $E_{hmax}$ on incident ion species.

*Photon-Induced Emission Measurements*

Total electron yield due to photon bombardment as a function of incident photon energy are also measured using the same hemispherical grid retarding field analyzer used for SE/BSE emission measurements. Again, this detector allows measurement of the energy spectra of the emitted electrons. The sample is biased to -20 eV to repel SE which would contaminate the emission measurements. The NIR-VIS-UV solar irradiance spectrum is simulated using a pair of monochromated lamp sources : (i) a Tungsten/halogen lamp system with a Suprasil envelope produces focused (~0.5 cm diameter) radiation from 0.4 eV to 7.2 eV (200 nm to 2000 nm) and (ii) a Deuterium RF powered continuum source with a $MgF_2$ window produces focused (~0.5 cm diameter) radiation from 3.1 eV to 11.1 eV (150 nm to 400 nm). Radiation from these sources passed through a nitrogen-purged monochromator [Sciencetech 200S]. A UV Si photodiode was calibrated against the pyroelectric detector as a UHV-compatible secondary intensity standard. NASCAP uses a single parameter, the total electron yield due to standard solar

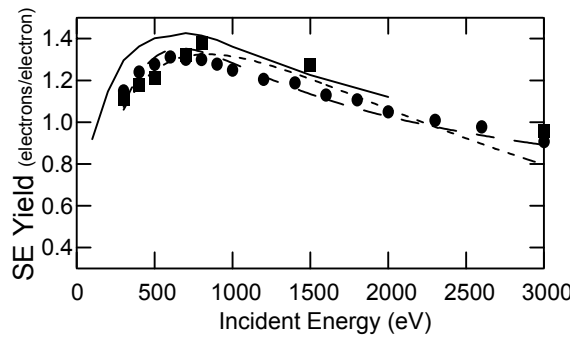


**Fig. 4.** Total SE yield vs incident energy for polycrystalline Ag.. Fits to the data for two models are shown.

irradiance, to characterize photon-induced electron emission. It is straightforward to determine this parameter from the measured spectra of electron emission versus incident photon energy, by normalizing for the solar spectral intensity [*Feuerbacher 1972*]. Photoelectron yield spectra are taken for possible use in updated charging codes.

## MATERIALS STUDIED

Based on extensive discussions with spacecraft charging community specialists, a set of conducting materials for investigation in this study have been proposed with the intent of meeting two objectives: (i) extending the NASCAP database to include the most common spacecraft materials currently in use and (ii) investigating representative materials with wide ranging physical properties. The accurate remeasurement of NASCAP parameters for those materials already incorporated in current NASCAP databases serves to confirm our experimental methods or update existing data which are not fully reliable.

A list of the proposed conducting materials is given in Table II. A number of elemental metals and common

Table II. Conducting Materials Proposed for Investigation

| Category | Sample Material |
|---|---|
| Elemental metals | Al*, Ag*, Au*, Be, Cu, Ti, Mg* |
| Alloys | Al 6061-T6, Al 2024-T3, Al 7075-T6, SS 316, Ti-6Al-4V |
| Semiconductors | Si, Ge, GaAs |
| Carbon materials | HOPG graphite, microcrystalline colloidal (Aquadag)*, soot, evaporated amorphous carbon, diamond-like amorphous carbon |
| Conductive coatings | Vapor-deposited ITO (In-Sn Oxide)* |

*Materials characterized in current NASCAP database [Mandell et al., 1993]

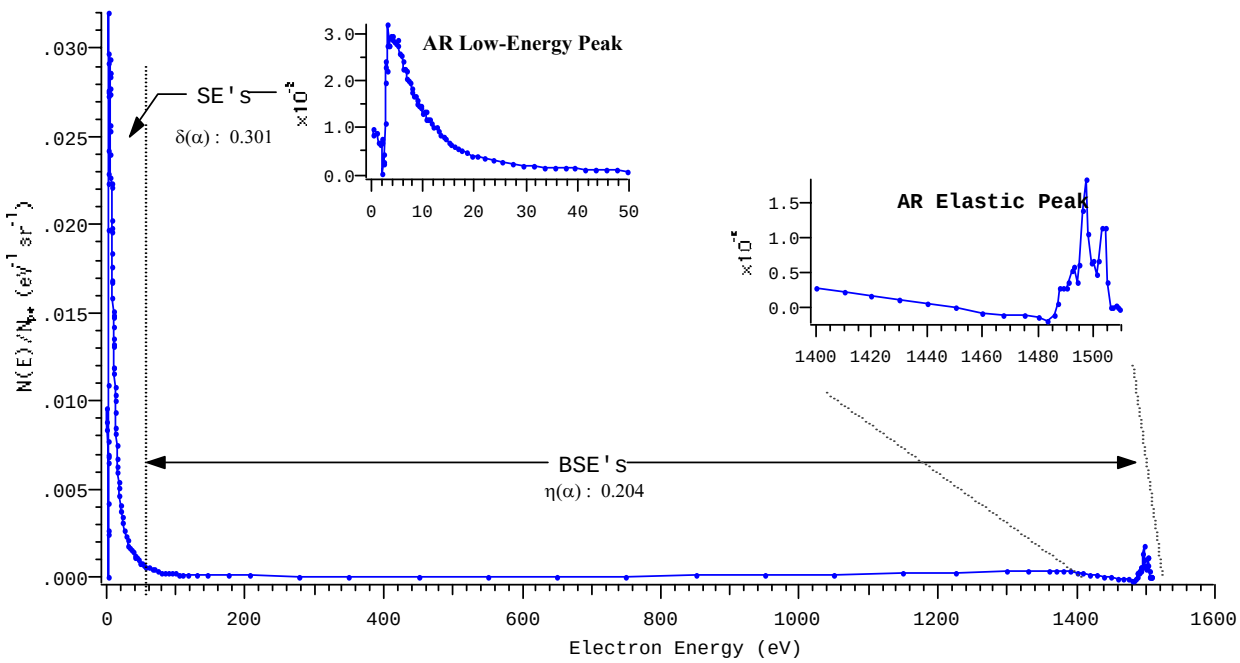


**Fig. 6.** Energy distribution of secondary and backscattered electrons at an emission angle of 17° and 1500 eV normal incident electron beam energy from a polycrystalline gold surface.

spacecraft alloys used as spacecraft structural elements are included. Semiconducting materials are common for solar arrays and sensors. A number of carbon materials will be studied. These materials, or similar materials, are often used in various aspects of spacecraft (e.g., carbon composites and thermal control surfaces). Their study is also essential to more fully characterize the effects of surface contamination ofspacecraft [*Davies and Dennison, 1997; Chang et. al, 2000*]. Indium-Tin-Oxide and carbon films are common conducting coatings often used with optics and sensor elements.

Materials for which measurements are completed are identified in Table II. Representative measurements of gold are described in the next section to illustrate typical results.

## REPRESENTATIVE MEASUREMENTS FOR GOLD

The high purity (4N) polycrystalline gold samples were cleaned chemically [*Davies, 1999*], inserted in the UHV chamber, annealed at 300 °C for ~50 hr, and ion sputtered with 500 eV argon ions at a fluence of ~5 mC·cm$^{-2}$. Optical microscopy, SEM and STM found a typical surface roughness of <2µm (see Fig. 2). AES mapping before and after electron emission measurements confirmed no measurable surface contaminants to a level of ~10% of a monolayer (see Fig. 3).

Figures 4 and 5 show the total SE yield and backscattered yield as functions of incident electron energy, respectively. Figure 6 shows the energy-resolved SE/BSE spectra for Au; the insets focus on the predominant SE and elastic peaks in the spectrum. Figure 7 shows an angular distribution of secondary electron emission. Figure 8 shows a comparison of the angular dependence of the BSE yield to theory.

## DISCUSSION

A Materials Report was prepared for each sample studied which contains a detailed description of the source of the sample, all measured characterization data, the raw data described in the section above, the derived values for NASCAP parameters and other models of the data, and a review of the available literature on the material [*Dennison, 2000*]. The parameters for NASCAP derived from the Au data in the previous section are listed in Table III.

## ACKNOWLEDGMENTS

The research described here was supported through a contract with the NASA Space Environment and Effects (SEE) Program. Instrumentation was funded primarily from the AFOSR (DURIP) Program and the USU Research Office [*Riffe,*

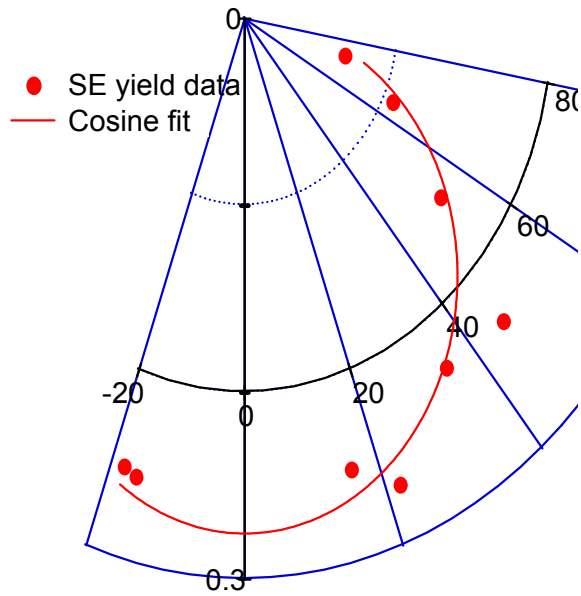


**Fig. 7.** Angular distribution of secondary electron yield at 1500 eV incident energy for argon sputtered polycrystalline gold.

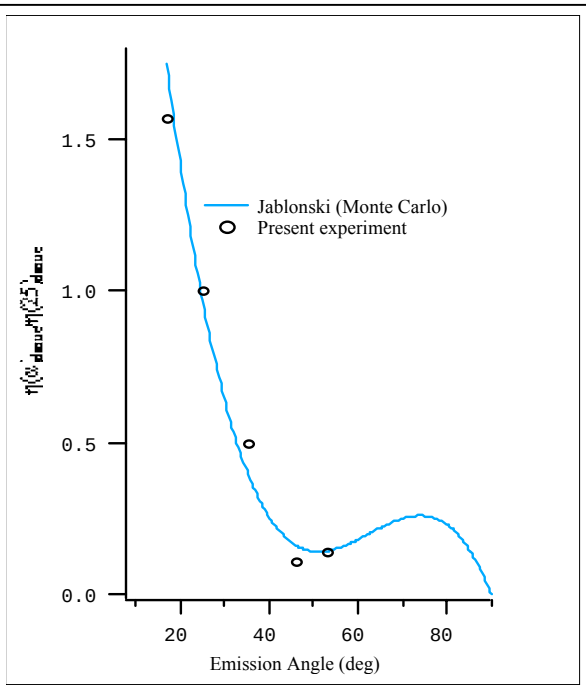


**Figure 8.** Comparison of angular distribution of elastic yield as computed by Joblonski [1991] and measured for polycrystalline Au at an incident energy of 1500 eV

Table III. NASCAP Parameters for Polycrystalline Au curves

| Parameter | Value |
|---|---|
| [1] Relative dielectric constant; $\epsilon_r$ (Input as 1 for conductors) | 1, NA |
| [2] Dielectric film thickness; d | $10^{-3}$ m, NA |
| [3] Bulk conductivity; $\sigma_o$ (Input as -1 for conductors) | $(3\pm1)\cdot10\cdot10^{7}$ $ohm^{-1}\cdot m^{-1}$ |
| [4] Mean atomic number <Z> | 79 (49.5±0.3) |
| [5] Maximum SE yield for electron impact; $\delta_{max}$ | 1.48±0.04 |
| [6] Primary electron energy for $\delta_{max}$; $E_{max}$ | (0.637±0.05) keV |
| [7-10] Fit to stopping power data; $b_1$, $n_1$, $b_2$, $n_2$ | $n_2$=1.35±0.04 $n_1 \ll 1$, $b_1 \ll b_2$, |
| [9 and 19] Density; ρ | $(1.932\pm0.002)\cdot 10^4$ $kg\cdot m^{-3}$ |
| [10] Mean atomic weight <A> | 196.97 |
| [11] SE yield due to proton impact $\delta^H$(1keV) | 0.413 |
| [12] Incident proton energy for $\delta^H_{max}$; $E^H_{max}$ | 135 keV |
| [13] Photoelectron yield, normally incident sunlight | $2.90\cdot10^{-5}$ $A\cdot m^{-2}$ |
| [14] Surface resistivity; $\rho_s$ | -1 ohm |
| [15] Max. potential before discharge to space; $V_{max}$ | 10000 V, NA |
| [16] Maximum surface potential difference before dielectric breakdown discharge; $V_{punch}$ | 2000 V, NA |
| [17, 18] Two parameter fit of radiation-induced conductivity, $\sigma_r$; k and Δ | NA |

NA -- Not applicable or approximated for bulk conductors.

*1996*]. Sample preparation and characterization was supported through an URCO grant from Utah State University (Judd).

## REFERENCES

Bedingfield, K.L., R.D. Leach and M.B. Alexander,: "Spacecraft System Failures and Anomalies Attributed to the Natural Space Environment." NASA Reference Publication 1390, NASA Marshall Space Flight Center, August 1996.

Cao, Y. and E.H. Conrad, Rev. Sci. Instrum. **60**, 2642 (1989).

W.Y. Chang, J.R. Dennison, Jason Kite and R.E. Davies, "Effects of Evolving Surface Contamination on Spacecraft Charging," Proceedings of the 38th American Insittute of Aeronautics and Astronomics on Aerospace Sciences, Reno, NV, January 12, 2000, in press.

W.Y. Chang, J.R. Dennison and Jason Kite, to be published, 2000.

W.Y. Chang, J.R. Dennison, Neal Nickles and R.E. Davies, "Utah State University Ground-based Test Facility for

Study of Electronic Properties of Spacecraft Materials," to be published in the *Proceedings of the 6th Spacecraft Charging Technology Conference*, (Air Force Research Laboratory Science Center, Hanscom Air Force Base, MA, 1999).

Chung, M.S. and T.E. Everhart, "Simple calculation of energy-distribution of low-energy secondary electrons emitted from metals under electron bombardment," J. Appl. Phys. **45**,2, 707-709, 1974.

Davies, R.E., "Measurement of Angle-Resolved Secondary Elctron Spectra," PhD Thesis, Utah State Univ., 1999.

Davies, R.E. and J.R. Dennison, *"Evolution of Secondary Electron Emission Characteristics of Spacecraft Surfaces,"* J. Spacecraft and Rockets , **34**, 571-574 (1997).

Davies, R.E.,"Backscattered and Secondary Electron Scattering Measurements with Applications to Spacecraft Charging," MS Thesis, Utah State Univ., 1996.

DeForest, S.E., J. Geophys. Res. **77**, 651 (1972).

Dennison, JR., "*Electronic Properties of Materials with Application to Spacecraft Charging: Year 1 Report,*" NASA Space Environments and Effects Program Grant, 2000.

Dennison, J.R., "*Electronic Properties of Materials with Application to Spacecraft Charging,*" NASA Space Environments and Effects Program Grant, 1998.

Dionnes, G.F., J. Appl. Phys. **46** 3347 (1975).

Feuerbacher and B. Fitton, J. Appl. Phys. **41** 1536 (1972).

Frooninckx, T., MS Thesis, Utah State Univ., 1991.

Frooninckz, T. and J.J. Sojka, J. Geophys. Res. **97**, 29851 (1992).

Gussenhoven, M.S. and E.G. Mullen, J. Spacecrafts and Rockets, **20**, 26 (1983).

Gussenhoven, M.S. *et al.* J. Geophys. Res., **90**, 11009 (1985).

Hastings, D. and H. Garrett, Spacecraft-environment Interactions, Cambridge University Press, 1996.

Katz, I., M. Mandell, G. Jongeward and M.S. Gussenhoven, J. Geophys. Res. **91**, 13739 (1986).

Leach, R.D. and M.B. Alexander.: "Failures and Anomalies Attributed to Spacecraft Charging," NASA Reference Publication 1354, NASA Marshall Space Flight Center, November 1994.

Mandell, M.J., P.R. Stannard and I. Katz, "NASCAP Programmer's Reference Manual," NASA Lewis Research Center, May 1993.

Mandell, private communications, 2000.

Nickles, N., R.E. Davies and J.R. Dennison, "Applications of Secondary Electron Energy- and Angular-Distributions to Spacecraft Charging," to be published in the *Proceedings of the 6th Spacecraft Charging Technology Conference*, (Air Force Research Laboratory Science Center, Hanscom Air Force Base, MA, 1999).

Riffe, D.M. and J.R. Dennison, "Ultra-high Vacuum Electron Scattering Chamber for the Characterization of Materials in Severe Environments, Surface and Nanocrystalline Solids," DOD-Defense University Research Instrumentation Grant, 8/1995-7/1996.

Schwarz, A., "Application of a semi-emperical sputtering model to secondary electron emission," J. Appl. Phys. **68** 2382 (1990).

Sternglass, E.J., "Theory of secondary electron emission by high-speed ions," Phys. Rev. **108**, 1, 1-12 (1957).